Development 138, 4351-4362 (2011) doi:10.1242/dev.065540

ApoE is required for maintenance of the dentate gyrus neural progenitor pool

Cui-Ping Yang[1,2], Jennifer A. Gilley[1,2], Gui Zhang[1,2] and Steven G. Kernie[1,2,*,†]

SUMMARY

Many genes regulating adult neurogenesis have been identified and are known to play similar roles during early neuronal development. We recently identified apolipoprotein E (*ApoE*) as a gene the expression of which is essentially absent in early brain progenitors but becomes markedly upregulated in adult dentate gyrus stem/progenitor cells. Here, we demonstrate that ApoE deficiency impairs adult dentate gyrus development by affecting the neural progenitor pool over time. We utilized ApoE-deficient mice crossed to a nestin-GFP reporter to demonstrate that dentate gyrus progenitor cells proliferate more rapidly at early ages, which is subsequently accompanied by an overall decrease in neural progenitor cell number at later time points. This appears to be secondary to over-proliferation early in life and ultimate depletion of the Type 1 nestin- and GFAP-expressing neural stem cells. We also rescue the proliferation phenotype with an ApoE-expressing retrovirus, demonstrating that ApoE works directly in this regard. These data provide novel insight into late hippocampal development and suggest a possible role for ApoE in neurodegenerative diseases.

KEY WORDS: Neurogenesis, Neural stem cell, Hippocampus, Mouse

INTRODUCTION

Despite intense interest in the implications of ongoing hippocampal neurogenesis, the mechanisms underlying its control remain primarily linked to what is known about developmental neurogenesis in other areas of the brain (Ding et al., 2008; Frederiksen and McKay, 1988; Seaberg and van der Kooy, 2002). Consequently, the majority of molecules shown to be essential for dentate gyrus development are most well known for neurogenesis that occurs during early brain development (Doetsch, 2003; Guo et al., 2008; Riquelme et al., 2008; Zhao et al., 2008). Molecules specific to neurogenesis within the more mature dentate gyrus remain elusive.

The maturation of the neuronal layers of the dentate gyrus occurs in a highly regulated manner; early Type 1 neural stem/progenitor cells (NSPCs) are slowly dividing and express both nestin and the astrocytic marker glial fibrillary acidic protein (GFAP) (Alvarez-Buylla et al., 2002; Encinas et al., 2006; Frederiksen and McKay, 1988). These cells give rise to the more rapidly dividing Type 2 neuroblasts that no longer express GFAP but express both nestin (Type 2a) and doublecortin (Type 2b) (Christie and Cameron, 2006; Duan et al., 2008; Gage, 2002; Peng et al., 2008; Seki, 2002; Seri et al., 2004). It is less common for the early Type 1 cells to give rise to mature astrocytes, suggesting that there are factors that regulate this pro-neuronal phenotype and make it distinct from earlier neuronal development in which the same original stem cell pool gives rise over time to astrocytic then oligodendrocytic precursors (Abrous et al., 2005; Kempermann et al., 2004; Tavazoie et al., 2008).

In order to address whether there might be molecules specific to the mature dentate gyrus that direct ongoing neurogenesis, we performed cell-specific cDNA arrays and identified several candidate genes that were differentially expressed between younger and older dentate gyrus progenitors (Gilley et al., 2011). One of the candidates most significantly upregulated later in development was the lipid and cholesterol regulator apolipoprotein E (*ApoE*). This gene has long been associated with neurodegenerative diseases that involve the hippocampus, though the mechanisms underlying this are unknown. Recently, ApoE has been implicated in dentate gyrus development during which its absence was observed to inhibit neurogenesis and increase the generation of astroctyes, something relatively rarely observed in the wild-type dentate gyrus (Li et al., 2009). Apolipoprotein E receptors are known to mediate dentate gyrus development by their binding to reelin, which regulates lamination of neuronal layers, though it appears that ApoE itself is dispensable for the early neuronal lamination that requires reelin (Herz and Beffert, 2000; Huang, 2009).

The purpose of the present study was to determine whether ApoE within this hippocampal progenitor niche plays a functional role in postnatal dentate gyrus development. Using loss-of-function mouse modeling, we confirmed its crucial role in late dentate gyrus development. Lack of ApoE allows early progenitors within the dentate to proliferate much faster than later-born progenitors expressing ApoE. In the absence of ApoE, neural progenitor cells are depleted over time as the increase in early proliferation results in depletion of the overall Type 1 pool of progenitors. We also demonstrate that this increased proliferation and subsequent depletion of Type 1 stem/progenitor cells ultimately gives rise to more astrocytes being generated within the mature dentate gyrus. These studies provide novel insight into both postnatal hippocampal development and the functional role of ApoE in neurogenesis.

[1]Department of Pediatrics, University of Texas Southwestern Medical Center, 5323 Harry Hines Blvd, Dallas, TX 75390, USA. [2]Department of Developmental Biology, University of Texas Southwestern Medical Center, 6000 Harry Hines Blvd, Dallas, TX 75390, USA.

*Present address: Departments of Pediatrics and Pathology and Cell Biology, Columbia University College of Physicians and Surgeons, 3959 Broadway, CHN 10-24, New York, NY 10032, USA
†Author for correspondence (sk3516@columbia.edu)

Accepted 8 August 2011

MATERIALS AND METHODS

Mice

All the mice were humanely housed and cared for in the Animal Resource Center (ARC) and the protocols were pre-approved by and conducted under the guidelines of the Institutional Animal Care and Use Committee (IACUC) at the University of Texas Southwestern Medical Center at Dallas. All the mice used for this work are wild-type and/or ApoE-deficient mice on C57/Bl6 background from Jackson Laboratory. These were crossed to pure C57/Bl6 nestin-GFP mice generated and extensively characterized by our laboratory containing a nestin-rtTA-eGFP (Chen et al., 2009; Gritti and Bonfanti, 2007; Miles and Kernie, 2008; Shi et al., 2007; Yu et al., 2005) or nestin-CreER^{T2} with loxp-stop-loxp yellow fluorescent protein (YFP) reporter mice from a wild-type or ApoE-deficient background (Blaiss et al., 2011; Chen et al., 2009; Li et al., 2008). Numbers of animals used are listed in the figure legends for each experiment.

Cell culture and proliferation analysis

All the neural progenitor cells were dissected from 600 μm coronal sections of wild-type or ApoE-deficient dentate gyrus, digested with activated papain solution containing 42 μl papain (Worthington), 27 μl of 100 mM cystein-HCl and 6 μl of 100 mM EDTA in 425 μl of DMEM/F12 and then grown in serum-free growth medium containing 20 ng/ml epidermal growth factor (EGF), 20 ng/ml fibroblast growth factor (FGF), 1% penicillin/streptavidin, 1% N2 supplement (Gibco), 1×B27 (Gibco) and 10 mg/ml heparin as previously described (Gilley et al., 2011). For the cell proliferation assay, neural progenitor cells were plated on poly-D-lysine- and laminin-coated plates and pulsed with 10 μM 5-bromo-2′-deoxyuridine (BrdU) for 15 minutes to label dividing cells in neural progenitor cell growth medium. Quantification of proliferation was performed manually in a blinded manner with Metavue or Image J software. To determine the cell proliferation in vivo, mice were given one pulse of BrdU at 100 mg/kg and 2 hours later the mice were perfused with 4% paraformaldehyde (PFA). One in every six sections (50 μm) were collected throughout the hippocampus and, after vibratome sectioning BrdU-specific immunohistochemistry with 3,3′-diaminobenzidine (DAB), staining was performed for analysis (see below).

RNA isolation and real-time PCR

Total RNA was isolated from either cultured neural progenitor cells or FAC-sorted GFP-positive cells with RNeasy Plus Micro Kit (Qiagen) and reverse transcribed to cDNA with SuperScript First-Strand Synthesis System for RT-PCR (Invitrogen). Suitable primers were added into the real-time PCR system together with the reverse transcribed cDNA and Faststart Universal SYBR Green Master (Roche). Real-time PCR was performed and quantified using the Applied Biosystems 7500 Real-Time PCR System software. The relative amount of tested genes was normalized to the internal control gene, GAPDH. Primer sequences for real time PCR were (5′-3′): ApoE Forward, TCCTGTCCTGCAACAACATCC, ApoE Reverse, AGGTGCTTGAGACAGGGCC; GAPDH Forward, CCATTCTCGGCCTTGACTGT, GAPDH Reverse, CTCAACTACATG-GTCTACATGTTCCA. Primers for reverse transcription and cloning were (5′-3′): ApoE Forward, CGCGTCGACATGAAGGCTCT, ApoE Reverse, CGGCGGCCGCTCATTGATTCTCCT. All primers were synthesized by Integrated DNA Technologies.

Immunohistochemistry

All animals were deeply anesthetized with ketamine and xylazine mixture before perfusion as described previously (Chen et al., 2009; Li et al., 2008; Miles and Kernie, 2008; Yu et al., 2008). After transcardial perfusion with ice-cold phosphate-buffered saline and 4% PFA, the whole brain was isolated, post-fixed overnight with 4% PFA, embedded in 3% agarose in PBS and sectioned with a vibratome (Leica Microsystems, VT1000S) at 50 μM intervals. All sections through the hippocampus were collected sequentially in 12-well plates. At least four free-floating sections with comparable anatomy were chosen from control animals and ApoE-deficient animals. All sections were permeabilized and blocked for at least 1 hour at room temperature with 0.3% Triton X-100 and 5% normal donkey serum in PBS. After the primary antibodies were incubated with the sections overnight at 4°C, sections were washed with PBS containing 0.3% Triton X-100 three times followed by incubation for 2 hours with secondary antibody in wash buffer containing 5% normal donkey serum at room temperature. For ApoE staining, the primary antibody was diluted in PBS containing 0.3% Triton X-100 and 0.02% NaN_3 for two full days at room temperature, then washed in wash solution three times and incubated with secondary antibody diluted in PBS for another two full days. After amplification with a Vectastain ABC Kit (Vector Laboratories), the signal was developed using a TSA plus Fluorescein or Cyanine 3 Evaluation Kit (PerkinElmer). For BrdU staining, all the sections were pretreated with 1 N HCl for 1 hour at 37°C to denature the DNA followed by 0.1 M borax (pH 8.5) treatment for 10 minutes to neutralize before the regular immunostaining procedure. Primary antibodies used were: rabbit anti-GFAP (DAKO, 1:1000), mouse anti-NeuN (Chemicon, 1:500), rabbit anti-GFP (Molecular Biology, 1:500), chicken anti-GFP (Aves, 1:500), goat anti-Dcx (Santa Cruz, 1:200), rat anti-BrdU (Abcam, 1:200), goat anti-ApoE (Millipore, 1:50,000), mouse anti-glutamine synthetase (Chemicon, 1:500) and goat anti-Iba-1 (Abcam, 1:150) All fluorescent-conjugated secondary antibodies (Cy2-, Cy3- or Cy5-anti-species) were used for confocal analysis (Jackson ImmunoResearch, all 1:200). All biotinylated-conjugated anti-species IgG were used for peroxidase/diaminobenzidine (DAB) staining for stereology analysis (Jackson ImmunoResearch, all 1:500).

Immunocytochemistry

All cells were fixed with 4% PFA for 15 minutes at room temperature, followed by immunocytochemical staining. The cells were blocked with 5% donkey serum in PBS containing 0.3% Triton X-100 for 1 hour, then incubated with primary antibody overnight at 4°C. After three washes with 0.3% Triton X-100 in PBS, samples were incubated with fluorescently conjugated secondary antibodies (Cy2-, Cy3- or Cy5- anti-species) and 4′,6-diamidino-2-phenylindole (DAPI) for 2 hours and coverslipped with immu-mount solution (Thermo Scientific). Primary antibodies used were: chicken anti-GFP (Abcam 1:1000), rat anti-BrdU (Abcam 1:500) and rabbit anti-GFAP (DAKO, 1:2000).

Flow cytometry

GFP-positive cells were sorted from the nestin-GFP transgenic mice as described previously (Gilley et al., 2011). Briefly, the whole dentate gyrus was microdissected from wild-type or ApoE-deficient hippocampus and dissociated with active papain as described for cell culture. After filtration with a 30 μm filter to remove undissociated tissue and debris, propidium iodide (PI, Sigma 1:1000) was added to each sample to exclude those dead cells 10 minutes before sorting. Cell sorting was performed with MoFlo (Beckman Coulter) and only GFP-positive cells were collected. Non-transgenic dentate gyrus was used as a negative control. For BrdU incorporation, cultured neural progenitor cells were pulsed with 10 mM BrdU for 15 minutes, dissociated manually, and single cells were fixed with ice-cold ethanol at 4°C for at least 30 minutes. After 30 minutes of room temperature treatment with 2 N HCl/Triton X-100 to denature the DNA and neutralization with 0.1 M $Na_2B_4O_7$ (pH 8.5), the cells were stained with APC-BrdU overnight and stained with PI before flow cytometry analysis. The analysis was performed on a FACSCalibur with lasers at 488 nm and 635 nm (BD Biosciences). For G_0 cell population isolation, we followed a method that has been widely used in hematopoietic stem cell separation and has been validated in neural stem/progenitor cells (Bersenev et al., 2008; Morrison et al., 1999; Shapiro, 1981). Here, we utilized Hoechst, a DNA-specific dye and pyronin Y, an RNA-specific dye, to distinguish the G_0 from G_1 population. Hoechst, an exclusive DNA dye, can distinguish the DNA content between 2C and 4C and G_0 and G_1 phase cells that have 2C DNA content. The quiescent cells, which are arrested in G_0 phase, have a lower level of RNA compared with active cells (G_1 phase). Therefore, Hoechst-negative/pyronin-negative cells represent low RNA and 2C DNA content, thereby defining the G_0 fraction. Cells were collected as above with FAC-sorting. After washing with 10% fetal bovine serum (FBS) in PBS once, 2 μg/ml Hoechst and/or 1 μg/ml pyronin Y were added into the samples and controls and incubated for 45 minutes at 37°C. Two washes with 10% FBS in PBS were performed before PI was added into the suspension samples and control. Samples were analyzed after being filtered with a 30 μm filter on MoFlo (Dako).

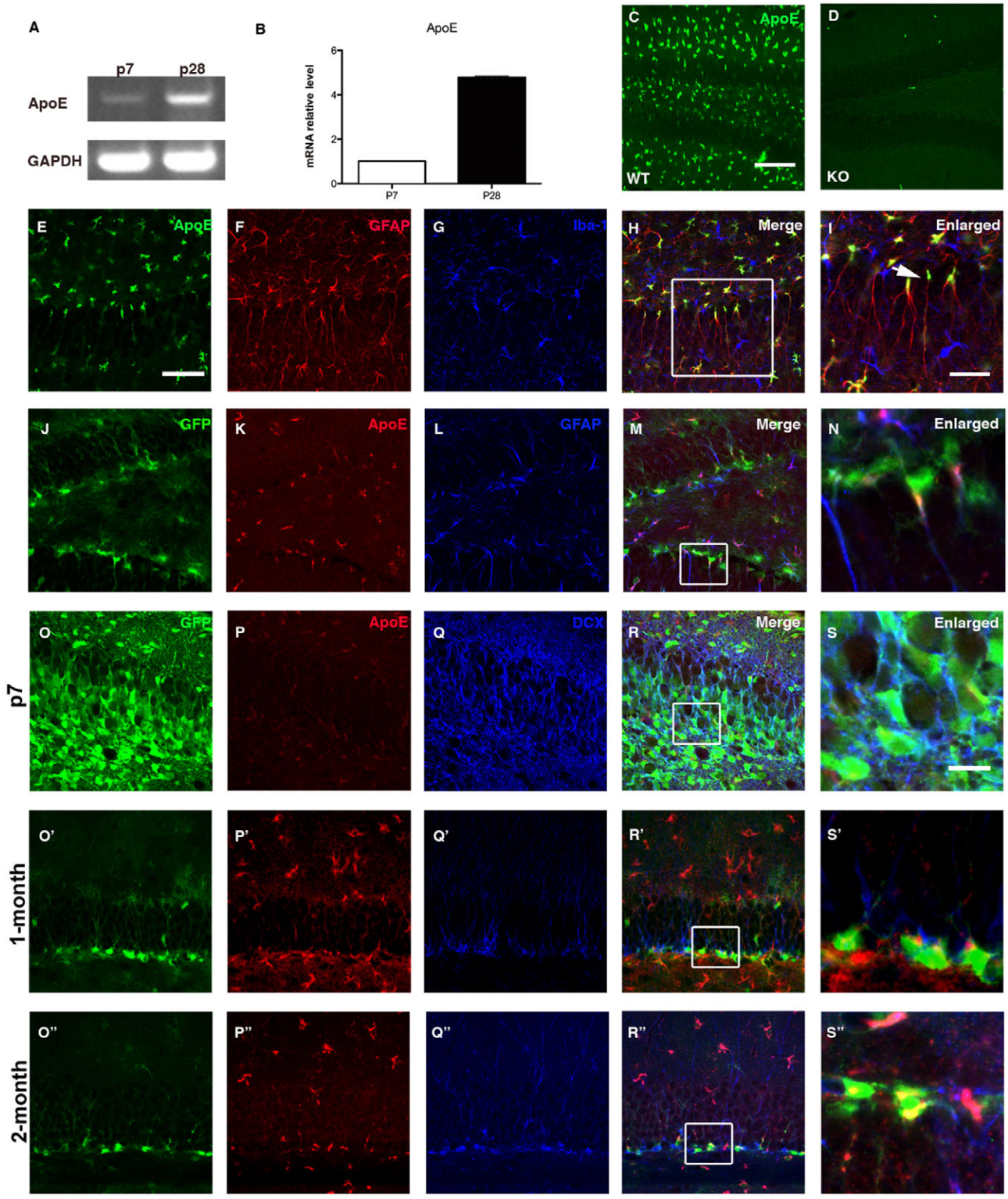

Fig. 1. ApoE is expressed in NSPCs and increases over time. (**A**,**B**) Reverse transcription and real-time quantitative PCR of ApoE from FAC-sorted NSPCs at P7 and 1 month of age (P28) demonstrate a greater than fourfold increase of ApoE in 1-month-old NSPCs. (**C**,**D**) Immunostaining of ApoE in the dentate gyrus from 1-month-old wild-type (WT; C) and ApoE-deficient (KO; D) mice show antibody specificity. (**E-H**) In 1-month-old wild-type animals, ApoE (green, E) colocalizes with the astrocytic and progenitor marker GFAP (red, F) within the dentate gyrus but not with the microglial marker Iba1 (blue, G). (**I**) Enlargement of the boxed area in H demonstrates that ApoE-expressing cells in the subgranular zone of the dentate gyrus contain GFAP-expressing long processes (arrows), indicative of early Type 1 stem cells. (**J-N**) ApoE (red, K) is expressed in nestin-GFP (green, J) and GFAP (blue, L) double-positive Type 1 NSPCs. N shows an enlargement of the boxed area in M. (**O-S″**) ApoE (red, P,P′,P″) is not detected in GFP-expressing (green, O) early neural progenitor cells at P7 (O-S) and Dcx-expressing (blue, Q,Q′,Q″) late neuronal progenitor cells (O-S″) but is apparent in GFP-expressing progenitors in 1- and 2-month-old animals (O′,O″). S, S′ and S″ show enlargements of the boxed areas in R, R′ and R″, respectively. Scale bars: 200 μm in C,E; 100 μm in I; 50 μm in S.

Confocal and stereology analysis

A Zeiss LSM 510 confocal multicolor microscope was used to determine the protein expression and the colocalization of immunohistochemical markers with Argon 488, Helium 543 and Helium 633 lasers and 40×/1.3 oil lens. To determine the GFP-, BrdU- and NeuN-positive cell numbers, we used an unbiased stereological approach (StereoInvestigator, Microbrightfield) for quantification on an Olympus BX51 System Microscope with a MicroFIRE A/R camera (Optronics). A one-in-six series of sections harboring the whole hippocampus in its rostrocaudal extension were immunostained with peroxidase/DAB and visualized under a light microscope and counted as described previously (Gilley et al., 2011). Briefly, The optical fractionator probe within the StereoInvestigator software (MBF Bioscience, MicroBrightField) utilized an unbiased counting frame (Gundersen, 1980; West, 1993) and was used to quantify cell number. Counting was performed using a 100× oil immersion lens. In addition, DAB sections stained for GFP were used to quantify the number of Type I cells in 1-month-old wild-type and ApoE knockout animals. Only Type I cells that exhibited the highly arborized dendritic tree morphology within the molecular layer of the dentate gyrus were counted (Lagace et al., 2007). For dentate gyrus volume quantification, the sections were stained with Nissl solution and estimated by Cavalieri Estimator.

S-phase length determination

Neural progenitor cells were cultured as a monolayer in poly-D-lysine- and laminin-coated 100 mm^3 plates. BrdU was dissolved in PBS and added to the culture medium at a final concentration of 10 μM for 15 minutes at 37°C. The cells were washed twice and further incubated at 37°C for 10 hours. Cells were isolated into single cells and fixed in 70% ice-cold ethanol after the PBS wash. After BrdU staining, cells underwent flow cytometry analysis. S-phase length calculation is based on a previously validated method (Eidukevicius et al., 2005).

Tamoxifen treatment in vivo

Tamoxifen (Sigma) was dissolved in sunflower oil (Sigma)/ethanol mixture (9:1) at 6.7 mg/ml. Vehicle or tamoxifen was injected intraperitoneally (IP) to mice at a concentration of 12.5 μl/g (0.83 mg/kg) twice a day for two consecutive days.

Statistical analysis

Statistical analysis was performed using Prism 5 software. *t*-tests (for paired data) or one-way ANOVA (for non-parametric) analysis with Bonferroni post-hoc correction were used for data analysis.

RESULTS

ApoE expression is specific to early neural stem/progenitors and increases over time

We previously generated and extensively characterized transgenic mice expressing enhanced green fluorescent protein (GFP) specifically within neural stem/progenitor cells (NSPCs) under the control of the neural progenitor-specific form of the nestin promoter and enhancer (Chen et al., 2009; Gritti and Bonfanti, 2007; Li et al., 2009; Li et al., 2008; Miles and Kernie, 2008; Shi et al., 2007; Yu et al., 2005; Yu et al., 2008). In addition, we recently demonstrated that ApoE expression increases dramatically from postnatal day (P) 7 to one month of age in GFP-expressing neural progenitor cells within the subgranular zone of the dentate gyrus (Gilley et al., 2011). To confirm these findings, we used flow cytometry to sort the GFP-expressing cells from P7 and 1-month-old nestin-GFP transgenic mice and determined the ApoE mRNA level with reverse transcription and real-time PCR (Fig. 1A,B). Both experiments show that ApoE RNA level was increased over fourfold in 1-month-old GFP-expressing NSPCs.

To address whether ApoE protein was also increased in older neural progenitor cells, we performed ApoE immunostaining. Using 1-month-old wild-type or ApoE-deficient coronal brain sections, we found that ApoE was expressed in a punctate, astrocyte-like pattern throughout the brain and its expression was absent in the ApoE-deficient hippocampus, validating its specificity (Fig. 1C,D). In order to determine the cell types expressing ApoE, we performed triple immunostaining and observed that the ApoE-expressing cells within the dentate gyrus expressed GFAP but not Iba1, demonstrating that ApoE was

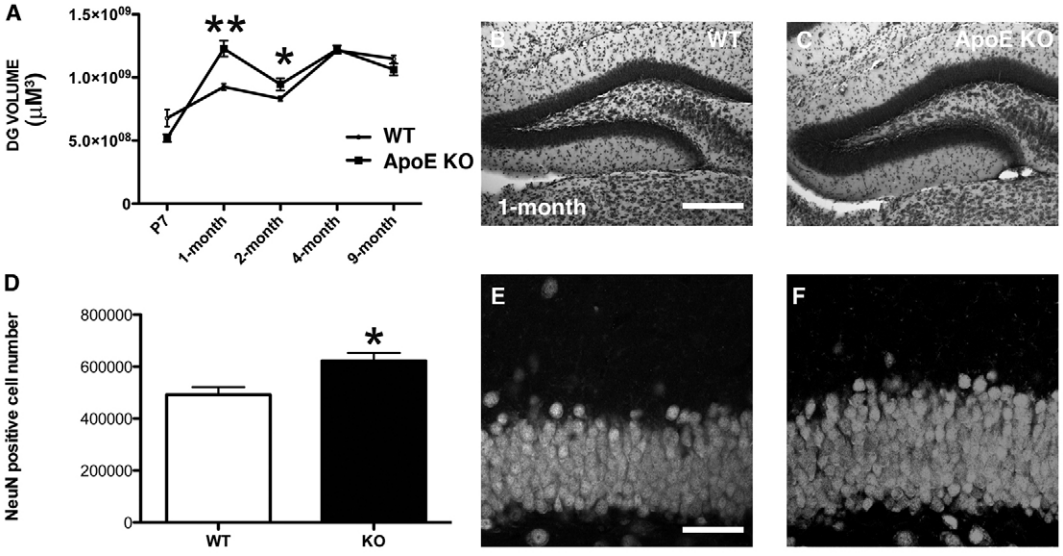

Fig. 2. Enlarged dentate gyrus (DG) in young ApoE-deficient mice. (**A**) DG volume quantification over time using three-dimensional volumetric reconstructions following Nissl staining. DG volume is significantly enlarged in ApoE-deficient mice (ApoE KO) compared with wild type (WT) at 1 and 2 months of age. (**B**,**C**) The DG granular layer at 1 month of age is enlarged in ApoE deficiency (C) compared with wild type (B). (**D**) Quantification of NeuN-positive mature neurons shows that there are more NeuN-positive neurons in ApoE deficient DG compared with wild-type DG. (**E**,**F**) The enlargement in the 1-month-old DG is due to increased cell number in ApoE deficiency (F) compared with wild type (E), as shown by NeuN staining. Data are derived from four animals per group (except the 4-month-old ApoE-deficient group in A, for which there are three animals). Error bars represent s.e.m. **P*<0.05, ***P*<0.01. Scale bars: 200 μm in B; 50 μm in E.

mainly expressed in astrocytes but not in microglia (Fig. 1E-I). In addition, its expression was found in the long GFAP-expressing processes within the subgranular layer of the dentate gyrus, typical for Type 1 early NSPCs (Fig. 1I, arrow). To confirm further that ApoE is expressed in Type 1 early neural stem/progenitor cells, we performed triple staining of GFP (green), ApoE (red) and GFAP (blue) (Fig. 1J-N) and found that ApoE localized to the GFAP-expressing processes of nestin-GFP-expressing early stem/progenitors. To confirm that ApoE is expressed in early progenitors and determine whether it was also expressed in later progenitors, we compared ApoE with GFP (for early neural progenitor cells), and doublecortin (Dcx) (for late neuronal progenitor cells) at P7, 1 month of age, and 2 months of age (Fig. 1O-S″). ApoE signal was barely detected at P7 though there was abundant GFP and Dcx (Fig. 1O-S). At 1 and 2 months of age, ApoE colocalized with GFP but not Dcx, demonstrating that its expression increases later in development than 1 month of age and within the progenitor niche (Fig. 1O′-S′).

To fully understand ApoE expression during the crucial period of P7 to 1 month of age, we examined several other time points (see Figs S1 and S2 in the supplementary material). As early as P14, we were able to detect ApoE expression in GFAP-positive early stem/progenitor cells, though the expression level was low and only a fraction of GFAP-expressing Type 1 cells expressed ApoE (see Fig. S1E-H in the supplementary material). As the dentate gyrus matured, more Type 1 cells expressed ApoE up to 2 months of age, when >95% of the Type 1 cells expressed ApoE (see Fig. S2F in the supplementary material). To characterize further the cell type of early neural progenitor cells that expressed ApoE, we analyzed ApoE expression in GFP/GFAP double positive Type 1 cells, GFP-positive Type 2 cells and GFP/BrdU double positive proliferating cells. ApoE was observed in the GFP/GFAP double positive Type 1 cells (see Fig. S2A-F in the supplementary material, arrow) whereas its expression in the GFP-positive Type 2 cells was very low and barely detectable (see Fig. S2E in the supplementary material, arrowhead). For the proliferating progenitors (GFP/BrdU double positive cells), we were unable to detect ApoE expression by immunostaining (see Fig. S2G-K in the supplementary material).

ApoE deficiency affects dentate gyrus development in a time-dependent manner

If ApoE plays a role in neuronal development, the dynamic expression pattern within the progenitor niche suggests different functional roles during the development of the dentate gyrus over time. We compared the dentate gyrus volume in ApoE-deficient mice with those of same-strain controls (C57/Bl6) over time using three-dimensional volumetric reconstructions using Nissl staining. From P7 to 1 month of age, when ApoE is not expressed highly in neural progenitor cells during normal development, there was a disproportionate growth in the neuronal layer of the dentate gyrus in the ApoE-deficient mice (Fig. 2A-C). This began normalizing at 2 months of age and up until 9 months of age, the dentate gyrus volume remained constant (Fig. 2A). We confirmed that these changes observed at 1 month of age were not due to increased neuronal size, but were

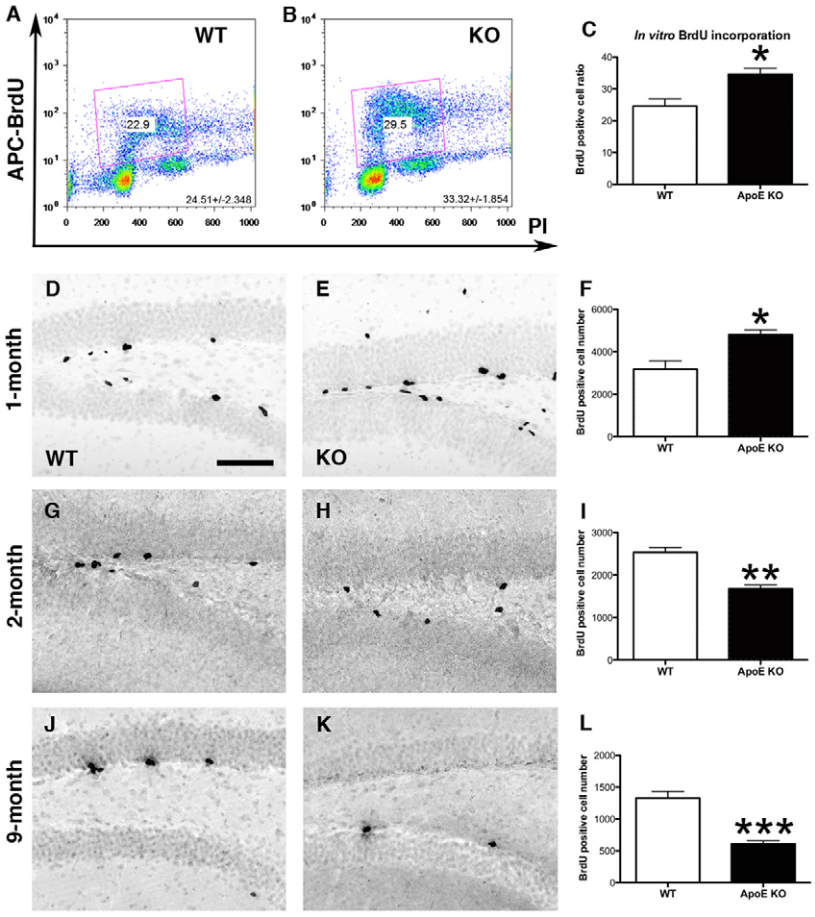

Fig. 3. Cell proliferation and progenitor number in vitro and in vivo in ApoE-deficient NSPCs. (**A**,**B**) In vitro BrdU incorporation is increased in ApoE-deficient NSPCs by flow cytometry analysis as indicated by number of PI-stained cells (*x*-axis) and number APC-BrdU-positive cells (*y*-axis). Colors represent relative cell number intensity (red>yellow>green>blue). Pink box outlines live cells expressing BrdU as quantified in C. (**C**) Statistical analysis of BrdU incorporation ratio between wild type and ApoE-deficiency derived from three independent experiments. Error bars represent s.e.m. **P*<0.05. (**D-L**) In vivo 2-hour BrdU incorporation demonstrates hippocampal dentate gyrus cell proliferation. In 1-month-old animals, BrdU incorporation is higher in ApoE-deficient mice (KO; E) than in wild-type mice (WT; D), whereas at 2 and 9 months of age, BrdU incorporation is decreased in ApoE-deficient mice (H,K) compared with age-matched wild-type controls (G,J). Statistical analysis of the difference between wild type and ApoE-deficiency is derived from at least five animals per group for 1- and 9-month-old animals (F,L) and three animals per group for 2-month-old animals (I). Error bars represent s.e.m. **P*<0.05, ***P*<0.01,****P*<0.001. Scale bar: 200 μm in D.

a result of increasing numbers of neurons by performing unbiased stereology on NeuN-expressing cells within the dentate gyrus (Fig. 2D-F). Thus, the growth of the neuronal layers of the dentate gyrus in ApoE deficiency was most apparent when much of dentate neurogenesis occurs between P7 and 1 month of age, but the normal expression of ApoE in neural progenitor cells at this time is typically low.

ApoE-deficiency increases early cell proliferation in the developing dentate gyrus but greatly diminishes over time

Because we observed increased growth of the dentate gyrus early during its formation, we investigated whether this was due to changes in proliferation using both in vitro and in vivo assays. In vitro, we used neurosphere cultures that were passaged at least three times from microdissected P7 dentate gyrus and, following a BrdU (10 μM) pulse, performed immunostaining quantification and flow cytometry analysis showing that there were more BrdU-positive cells incorporated in ApoE-deficient neurospheres (Fig. 3A-C). We also injected BrdU (100 mg/kg) in both wild-type and ApoE-deficient mice at different postnatal ages. Similar to the age-dependent changes that we observed in dentate gyrus volume (Fig. 2), we observed more BrdU-positive cells in the ApoE-deficient dentate gyrus compared with wild type in 1-month-old animals (Fig. 3D-F). However, BrdU-positive cells decreased dramatically in the ApoE-deficient dentate gyrus compared with wild type in 2- and 9-month-old animals (Fig. 3G-L). At 2 months of age, BrdU incorporation in ApoE-deficient mice was ~66% of that seen in wild type, whereas at 9 months of age, it was only ~42% of that seen in the wild type.

To understand whether increased BrdU incorporation in ApoE-deficient dentate gyrus is due to the lengthening of S-phase or not, we measured the S-phase length of wild-type and ApoE-deficient neural stem and progenitor cells in vitro based on a validated protocol (Eidukevicius et al., 2005). We observed no differences in S-phase length between wild-type and ApoE-deficient neural progenitors (see Fig. S3 in the supplementary material).

Neural stem/progenitors decrease over time in ApoE deficiency

We next determined, using unbiased stereology, what happened to the GFP-expressing progenitors within the dentate gyrus over time. As noted above, the BrdU-incorporated cell number in the ApoE-deficient dentate gyrus was increased at 1 month of age whereas the number of GFP-expressing progenitors was similar (Fig. 4A-C). Thus, although the proliferation rate was higher in the ApoE-deficient dentate gyrus, the number of progenitors was unchanged at 1 month of age, which is consistent with the in vitro BrdU incorporation assay (Fig. 3A-C). At 2 months of age, however, the GFP-expressing progenitor cell number decreased by ~25%, consistent with fewer BrdU-expressing cells as well as a decrease in dentate gyrus volume (Fig. 4D-F, Fig. 3G-I and Fig. 2A). Comparing wild-type and ApoE-deficient dentate gyrus, the most dramatic difference in GFP-expressing cell number was observed in 9-month-old animals. We observed that, overall, GFP-expressing cells were decreased when compared with earlier time points and the number was even less in the ApoE-deficient dentate gyrus (Fig. 4G-I). Thus, decreases in proliferation that occurred after 4 weeks of age were accompanied by an eventual decline in neural stem/progenitors when ApoE was absent from these cells.

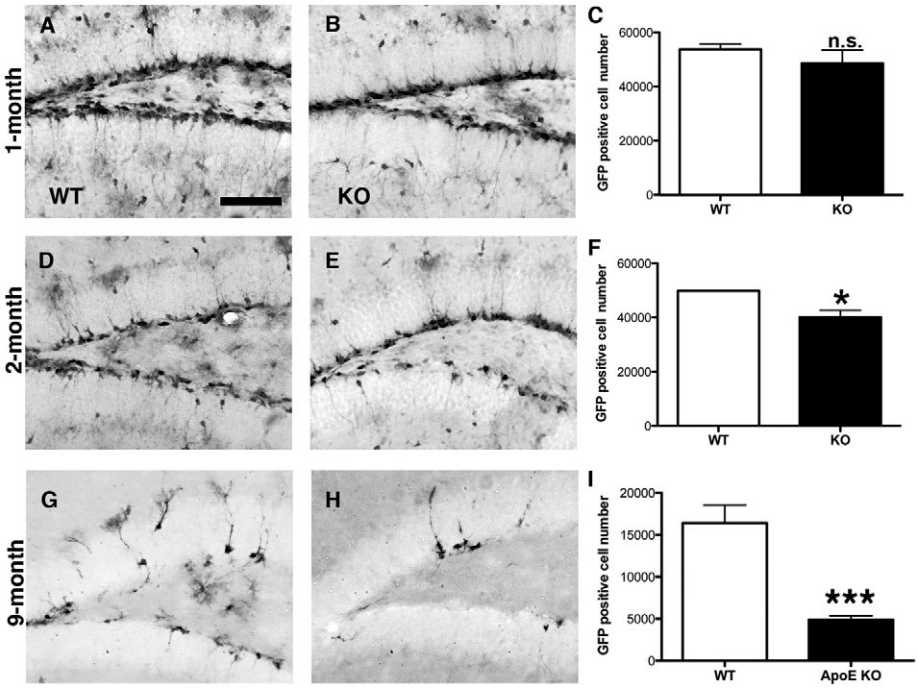

Fig. 4. GFP-expressing neural progenitor cell number decreases over time. (**A-C**) Neural stem/progenitor cell (GFP-expressing cell) number is comparable in wild-type (WT; A) and ApoE-deficient (KO; B) dentate gyrus at 1 month of age using unbiased stereological quantification in nestin-GFP transgenic mice. n.s., non-significant. (**D-I**) Neural stem/progenitor cell number is decreased in the ApoE-deficient (E,H) dentate gyrus at 2 and 9 months of age compared with age-matched wild type (D,G). Statistical analysis is derived from four animals per group at 1 (C) and 9 (I) months of age and three animals per group at 2 months of age (F). Error bars represent s.e.m. *P<0.05, ***P<0.001. Scale bar: 100 μm in A.

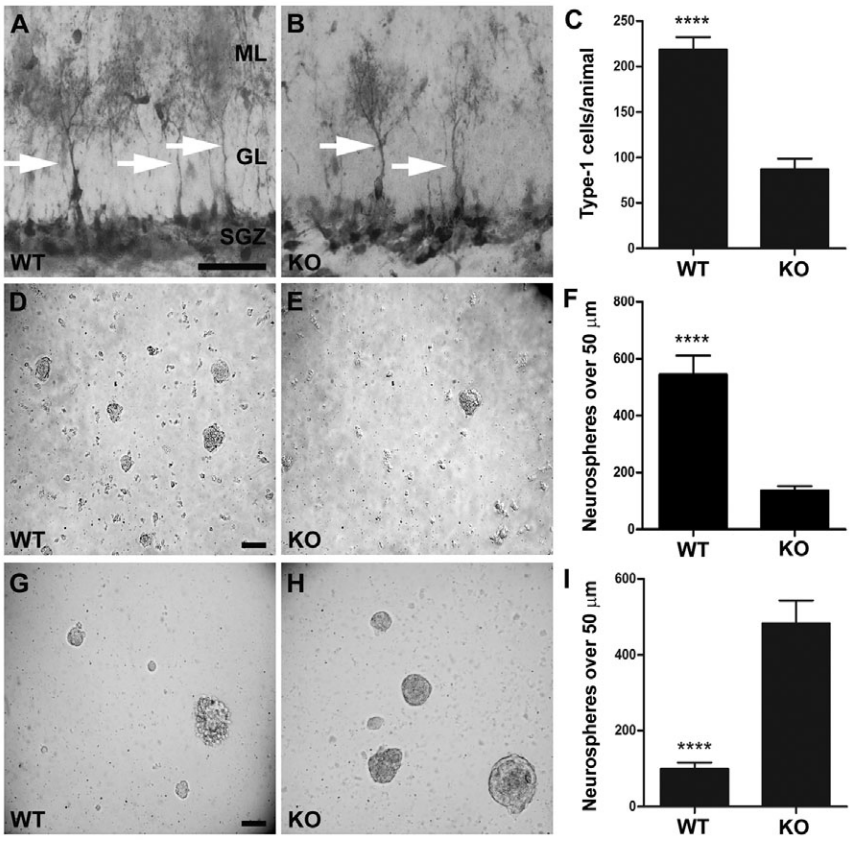

Fig. 5. Type 1 cells regulate progenitor proliferation and self-renewal capacity. (**A-C**) The number of Type 1 cells (arrows) is decreased in ApoE-deficient mice (KO; B) compared with wild-type controls (WT; A). (**D-F**) Primary neurosphere cultures derived from the dentate gyrus of 1-month-old wild-type (D) and knockout (E) mice show that neurosphere formation is decreased in progenitors lacking ApoE. (**G-I**) Passaged neurospheres from wild-type (G) and knockout (H) animals indicate that ApoE-deficient progenitors have an increased capacity for self-renewal. Statistical analysis utilized an unpaired *t*-test to determine significance. ****$P<0.0001$. $n \geq 4$. Error bars represent s.d. Scale bars: 35 μm in A; 50 μm in D,G.

Decreased number of Type 1 cells in ApoE deficiency affects proliferation and the capacity to self-renew in vitro

Although the total number of GFP-expressing progenitors was similar at 1 month of age (Fig. 4A-C), we further determined the number of early Type 1 stem/progenitor cells within this population. In order to do this, we utilized cell morphology to quantify the number of Type 1 cells within the dentate gyrus of 1-month-old wild-type and ApoE-deficient mice. We observed only 40% as many Type 1 cells in 1-month-old ApoE-deficient animals compared with wild-type controls (Fig. 5A-C). These results suggest that, although the number of GFP-expressing cells at this time point might not be different, the number of Type 1 progenitors is already being exhausted in ApoE-deficient mice.

These discrepancies in the number of Type 1 cells led us to examine their growth potential in vitro. Using cells derived exclusively from the dentate gyrus of 1-month-old wild-type and ApoE-deficient animals, we assayed their ability to proliferate and form primary neurospheres for three weeks in culture in semi-solid media. The number of neurospheres over 50 μm in diameter was quantified and there were significantly more of these neurospheres derived from the wild-type dentate gyrus when compared with the ApoE-deficient mice (Fig. 5D-F). These results indicate that the decreased number of Type 1 progenitors in 1-month-old ApoE-deficient animals diminished the number of primary neurospheres generated in vitro.

We next analyzed the ability of these progenitor cells to self-renew. To do this, we performed a single passage on wild-type and ApoE-deficient neurospheres derived from 1-month-old animals and quantified the number of new neurospheres formed in vitro. Although we demonstrated fewer primary neurospheres in ApoE-deficiency, by passaging them we could observe the ability of individual progenitors to form neurospheres. Interestingly, these clonal assays from passaged cells lacking ApoE were able to form nearly five times more neurospheres than progenitors from wild-type cells did (Fig. 5G-I). Thus, Type 1 cells lacking ApoE exhibited increased self-renewal, which is consistent with results showing increased BrdU incorporation in ApoE deficiency (Fig. 3D-F).

Type 1 early stem/progenitors are permanently depleted in the absence of ApoE

Because GFP expression is controlled by the nestin promoter and both Type 1 (stem) and Type 2 (committed progenitor) cells express nestin, it is unclear whether the decline of neural stem/progenitors occurs primarily in the progenitor cell population or is the consequence of depletion of the neural stem cell pool. To distinguish between these two possibilities, we stained neural stem/progenitor cells with an RNA-specific dye, Pyronin Y (Py), in conjunction with a DNA-specific dye, Hoechst 33342 (Ho), to differentiate the G_0 from the G_1 population. $Py^- Ho^-$ represents low RNA content and 2C DNA content, thereby defining the G_0 fraction (Bersenev et al., 2008).

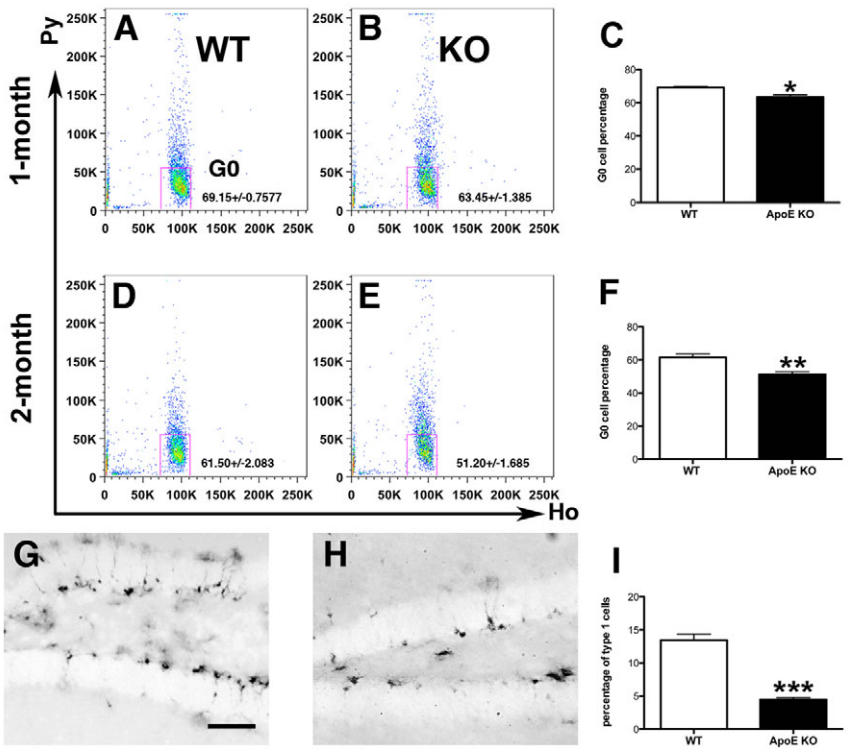

Fig. 6. Neural stem cell number decreases over time. (**A-F**) G_0 neural stem cell numbers are lower in ApoE-deficient (KO; B,E) compared with wild-type (WT; A,D) mice at 1 and 2 months of age using flow cytometry analysis stained with pyronin Y (pY, *y*-axis) and Hochest (Ho, *x*-axis). See Fig. 3A,B for explanation of graphs. (**G-I**) At 9 months of age, Type 1 cell number decreases even more dramatically in ApoE-deficient (H) compared with wild-type (G) mice, as determined by the quantification of typical Type 1 cells based on the cell morphology stained with GFP. The statistical analysis for flow cytometry results are derived from at least four animals per group (C,F) and for cell count quantification from four animals per group (I). Error bars represent s.e.m. **P*<0.05, ***P*<0.01, ****P*<0.001. Scale bar: 100 μm.

At 1 month of age, both wild-type and ApoE-deficient mice contained >60% G_0 cells, which are believed to be quiescent Type 1 cells, whereas in the ApoE-deficient dentate gyrus there were fewer G_0 cells compared with wild type (Fig. 6A-C). As we observed no significant difference in GFP-expressing cells between the wild-type and ApoE-deficient dentate gyrus, the Type 2 committed progenitor population was, therefore, higher in the ApoE-deficient dentate gyrus, which is consistent with the BrdU incorporation experiments in vivo. At 2 months of age, both the GFP-expressing and the G_0 cell populations decreased more significantly in the ApoE-deficient dentate gyrus (Fig. 6D-F and Fig. 4D-F). Because Type 2 cells arise from the Type 1 early progenitors, it appears that the overall decrease observed in the GFP population is the consequence of depleted neural stem cells. At 9 months of age, the GFP-expressing Type 1 cells decreased even more dramatically than at 2 months of age. The quantification of the Type 1 cell was analyzed by cell morphology with DAB staining because at this age there are not enough cells to perform flow cytometry (Fig. 6G-I).

In the absence of ApoE, Type 1 early stem/progenitors retained an increased proliferative phenotype

Over time, the GFP-expressing progenitors were diminished in both the wild-type and ApoE-deficient dentate gyrus. Because the absence of ApoE confers increased proliferative potential early in development we wanted to test whether this increase in proliferation was maintained even when the overall pool was depleted. At 1 month of age, we observed twice the percentage of early Type 1 progenitors dividing in ApoE deficiency (Fig. 7A-C). This was not surprising as the overall proliferation at this time point was increased in the ApoE-deficient state (Fig. 3D-F). However, we also observed similar increases in BrdU-expressing Type I early progenitors in both 2- and 9-month-old animals (Fig. 7D-I); the later time points are when the overall number of dividing progenitors was substantially decreased in the ApoE-deficient state (Fig. 3G-L). This suggests that the increased proliferation observed in ApoE deficiency persists throughout the lifespan though the overall pool becomes depleted.

Replacement of ApoE rescues the ApoE-deficient proliferation phenotype

The expression of ApoE is most prominently observed in both astrocytes and progenitor cells (Fig. 1). To determine whether the proliferation was directly related to ApoE deficiency, we performed a rescue experiment by retroviral expression of wild-type ApoE in ApoE-deficient neural progenitor cells. Compared with control (GFP-only) retrovirus-infected ApoE-deficient neural progenitor cells, cells infected by retroviral-ApoE had less BrdU incorporation (Fig. 8C,D,F). A similar phenotype was represented in the retrovirus-infected wild-type neural progenitor cells (Fig. 8A,B,E). To characterize further whether there was any paracrine effect of ApoE on adjacent cells, we analyzed the cell proliferation of those non-transfected cells in the same dish with ApoE-deficient neural stem/progenitor cells. The non-transfected cells had a similar proliferative ability as the GFP-only transfected cells; thus, there was no apparent paracrine effect between the transfected and non-transfected cells (Fig. 7G). Therefore, the increased proliferation of neural progenitor cells observed in ApoE deficiency was a direct effect of loss of ApoE.

ApoE deficiency increases hippocampal astrocyte formation in vivo

The normalization of the neuronal layer of the dentate gyrus in ApoE deficiency over time and the recently reported role of ApoE in directing progenitor fate in mature progenitors suggested that late-born progenitors might be preferentially becoming astrocytes (Li et al., 2009). To assay for this in vivo, we used ApoE-deficient

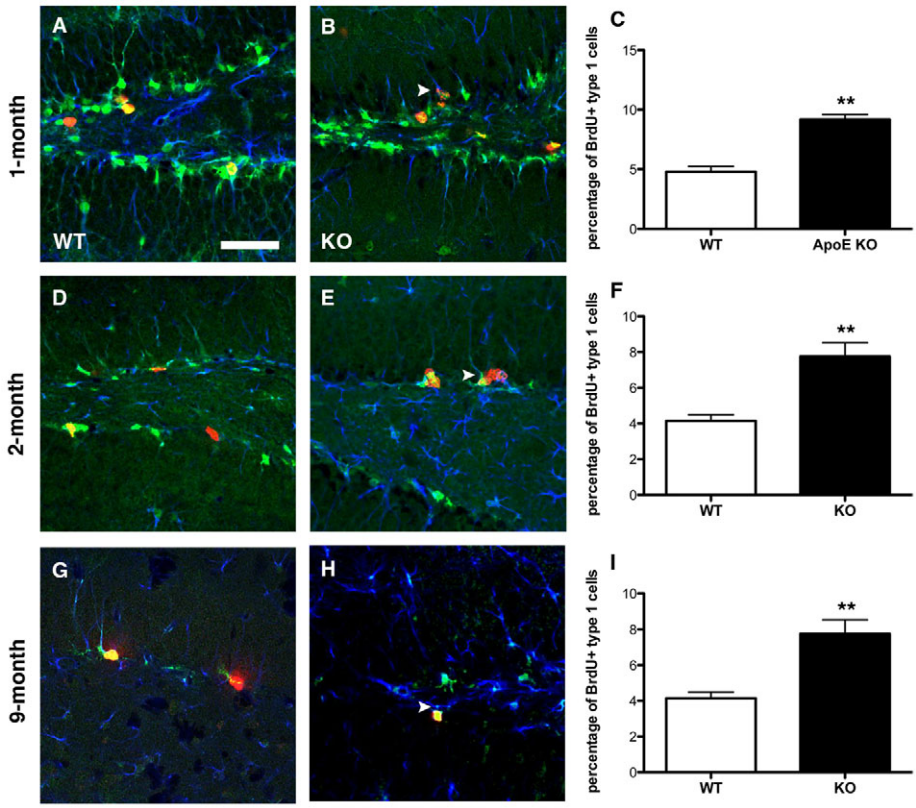

Fig. 7. Dividing Type 1 cells are increased in ApoE deficiency over time.
(**A-I**) Although the number of progenitors decreases over time during normal aging and in ApoE deficiency, there remain increased numbers of Type 1 early progenitors (GFP-positive, green; GFAP-positive, blue) that colocalize with BrdU (red). Statistical analysis is derived from at least three animals per group at 1 (C) and 9 (I) months of age and four animals per group at 2 months of age (F). Error bars represent s.e.m. $^{**}P<0.01$. Scale bar: 100 μm.

mice crossed with nestin promoter/enhancer-driven inducible Cre-recombinase (nestin-CreER^{T2}) and ROSA26 loxp-stop-loxp yellow fluorescent protein (YFP) reporter mice (Blaiss et al., 2011; Chen et al., 2009; Li et al., 2008). Mice were injected with tamoxifen at 2 weeks of age and sacrificed at 6 weeks of age then immunostained with the astrocyte-specific marker glutamine synthetase (GS) to distinguish GFAP-expressing mature astrocytes from GFAP-expressing early Type 1 neural stem/progenitor cells (Miles and Kernie, 2008; Blaiss et al., 2011). They were also stained with the neuronal marker NeuN and the lineage marker YFP. We found more than double the number of GS-expressing astrocytes in the ApoE-deficient dentate gyrus that expressed the lineage marker YFP compared with observations in wild-type controls (Fig. 9A-J). These in vivo data demonstrate that ApoE deficiency led to more astrocytic differentiation of hippocampal neural stem/progenitor cells.

DISCUSSION

Numerous studies have addressed mechanisms underlying adult mammalian neurogenesis since Altman first demonstrated that new neuronal-appearing cells were found in the brains of adult rats and cats (Altman and Das, 1965). The use of bromodeoxyuridine (BrdU) and the evidence for BrdU-labeled cells in the adult human hippocampus has stimulated much more recent and intense investigation in this area (Cameron and McKay, 2001; Eriksson et al., 1998; van Praag et al., 2002; Zhao et al., 2006). The now well-accepted notion of ongoing adult neurogenesis has opened a new field for the treatment of injury and neurodegenerative diseases in the adult brain, though the mechanisms underlying this phenomenon are just beginning to emerge (Kim and de Vellis, 2009; Lindvall and Kokaia, 2010).

Recent studies indicate that multiple signaling pathways are involved in regulating both early brain development and adult neurogenesis, whereas the unique signals regulating adult neurogenesis are mostly unknown and have been minimally investigated (Ming and Song, 2005; Suh et al., 2009). For example, the sonic hedgehog and bone morphogenetic (BMP) signaling pathways are crucial for both embryonic and adult neurogenesis (Joksimovic et al., 2009; Lai et al., 2003; Machold et al., 2003; Pfrieger, 2003b; Slezak and Pfrieger, 2003). Here, we demonstrate that ApoE is minimally expressed during early development within the progenitor population, but as its expression increases in the adult, it becomes required for proper ongoing hippocampal development and maintenance.

ApoE is a major apolipoprotein and a cholesterol carrier in the central nervous system (Mahley, 1988). It is mainly expressed in astrocytes in the brain and is only expressed in neurons in response to excitotoxic injury (Xu et al., 2006). In the brain, cholesterol is an essential component of membranes and myelin sheaths, and is crucial for synaptic integrity and neuronal function. Cholesterol is transported mainly from astrocytes to neurons and ApoE plays fundamental roles in this process (Pfrieger, 2003a; Pfrieger, 2003b). Because of the importance of cholesterol in brain development, there are many neuronal functions that could be influenced by changes in ApoE. These include migration, axon guidance, microtubule stability, survival, amyloid deposition, regeneration and synaptic plasticity (Beffert et al., 2004; Bu, 2009; Herz and Beffert, 2000). All of these functions, however, are attributed to the major ApoE receptors (ApoER2 or VLDLR) that are expressed in neurons and bind other ligands, such as reelin (Deguchi et al., 2003; Kim et al., 1996; Trommsdorff et al., 1999).

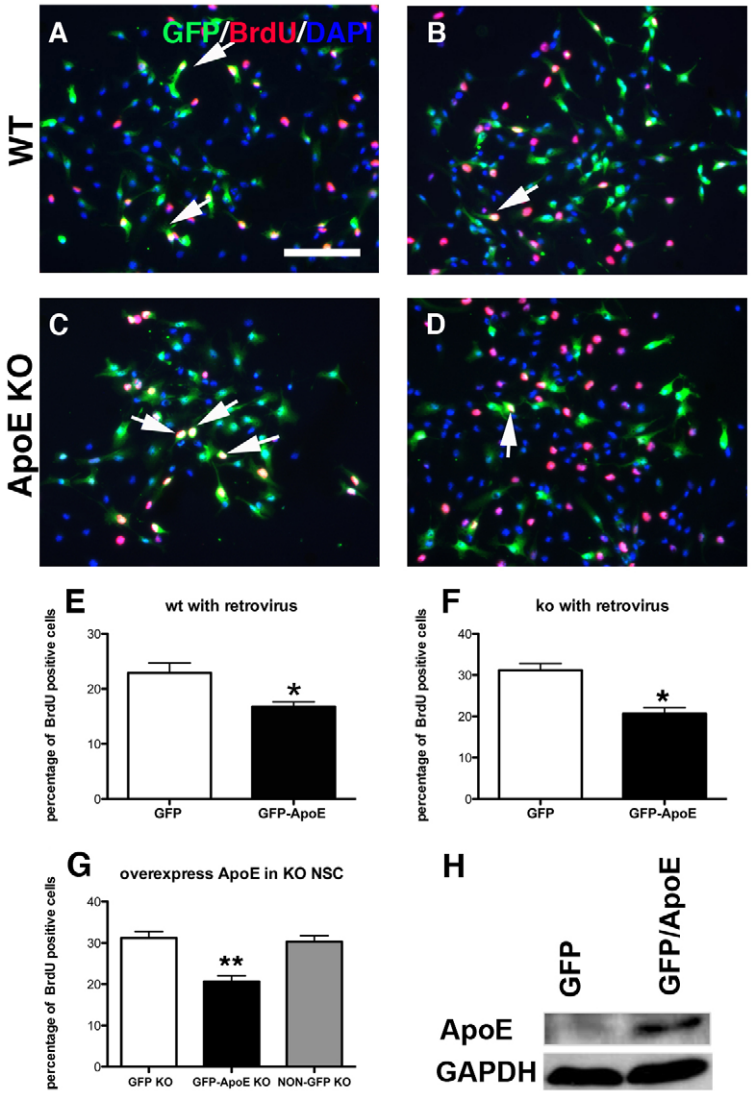

Fig. 8. Abnormal cell proliferation in ApoE deficiency can be rescued with an ApoE-expressing retrovirus. (**A-D**) Cell proliferation is further decreased after ApoE was re-expressed in wild-type (WT) and ApoE-deficient (ApoE KO) NSPCs. More triple-stained nuclei (arrows) are observed following infection with GFP-only-expressing retrovirus (A,C) than following infection with retrovirus expressing both GFP and ApoE (B,D). (**E**,**F**) Quantification of BrdU incorporation after retrovirus infection in wild-type (E) and ApoE-deficient (F) NSPCs. (**G**) No paracrine effect of ApoE is observed in non-infected neural progenitor cells. BrdU incorporation in non-GFP cells was quantified and compared with GFP only and GFP/ApoE-infected cells. (**H**) Western blot demonstrates that ApoE is re-expressed in ApoE-deficient NSPCs after infection with GFP/ApoE retrovirus. Statistical analyses are derived from three independent experiments. Error bars represent s.e.m. **P*<0.05, ***P*<0.01. Scale bar: 100 μm.

The present study demonstrates that ApoE directs adult hippocampal development within the neural stem/progenitor niche. In the early development of the dentate gyrus, ApoE expression level is low and the neural stem and progenitor cells quickly proliferate and differentiate into the granular neurons of the dentate gyrus. When the dentate gyrus is more fully formed at 1 month of age, ApoE expression increases and inhibits neural stem/progenitor cell proliferation and maintains the progenitor cell precursor characteristics. Here, we have demonstrated that when ApoE is deficient, progenitor cells keep proliferating at a high frequency until the progenitor pool becomes depleted, whereas the numbers of astrocytes derived from neural stem/progenitor cells are increased. This phenotype is consistent with observations from two recently published and apparently oppositional studies on the dentate gyrus progenitor niche (Bonaguidi et al., 2011; Encinas et al., 2011). Encinas et al. propose a disposable stem cell model whereby the stem cell pool itself is limited and the final progenitor division ultimately gives rise to a mature astrocyte (Encinas et al., 2011). The present work supports this model, but it is also consistent with the notion that increasing proliferation within the early Type 1 progenitor cells ultimately leads to generation of more astrocytes (Bonaguidi et al., 2011). Thus, taken together these data establish that ApoE is essential for inhibiting cell proliferation, maintaining neural precursor characteristics and promoting neurogenesis.

Many recent studies suggest that adult neural stem cells are derived directly from radial glia and are themselves a specific subpopulation of astrocytes (Gritti and Bonfanti, 2007; Kriegstein and Alvarez-Buylla, 2009). ApoE is a molecule that is mainly secreted by astrocytes and is thought to be an astrocyte-specific marker (Fujita et al., 1999). The fact that ApoE is expressed in both Type 1 neural progenitor cells and astrocytes further validates the glial nature of neural stem cells. ApoE has long been implicated in a variety of neurodegenerative processes that affect hippocampal function. Recent data demonstrate that it also has dentate gyrus-specific effects, including directing progenitor fate towards astrocytic lineages (Bu, 2009; Li et al., 2009). This present work demonstrates that ApoE actually plays a dual role in dentate gyrus development. In the early development of the dentate gyrus, ApoE expression is strictly controlled and its lack of expression in neural stem cells allows these precursor cells to quickly proliferate and differentiate. When it does become expressed within the progenitor population later on, it clearly directs ongoing development, which suggests that ApoE is an important regulator that helps balance

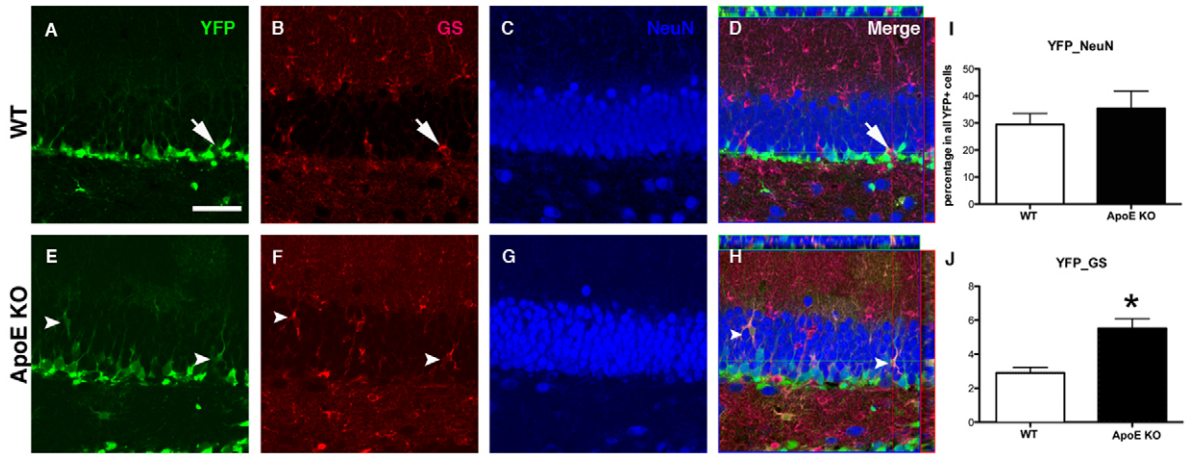

Fig. 9. Neural progenitor cells differentiate into astrocytes more often in ApoE-deficient mice. (**A-J**) In vivo cell differentiation analysis with progenitors from wild-type (WT; A-D) and ApoE-deficient (ApoE KO; E-H) dentate gyrus in animals that were crossed with a nestin-CreER^{T2} transgenic and a floxed ROSA-26 YFP reporter. P14 animals were injected with tamoxifen and cell fate was tracked after 1 month. YFP-expressing cells within the dentate gyrus were more than double that observed in the control animals (J). Arrow (A,B,D) highlights a glutamine synthetase (GS)-expressing astrocyte that does not express YFP. Arrowheads (E,F,H) indicate GS-expressing astrocytes that also express YFP, signifying astrocytes derived from nestin-expressing neural progenitor cells. Statistical analysis was derived from three animals per group. Error bars represent s.e.m. **P*<0.05. Scale bar: 50 μm.

hippocampal progenitor cell fate. This, therefore, provides an additional mechanism whereby human *ApoE* polymorphisms might contribute to hippocampal neurodegenerative diseases that do not become apparent until late in life.

Acknowledgements
We are grateful to Jenny Hsieh for providing experimental advice.

Funding
Financial support is from NIH grant R01 NS048192 (to S.G.K.) and the Sarah M. and Charles E. Seay Endowed Fund for Research on Brain and Spinal Cord Injuries in Children. Deposited in PMC for release after 12 months.

Competing interests statement
The authors declare no competing financial interests.

Supplementary material
Supplementary material for this article is available at
http://dev.biologists.org/lookup/suppl/doi:10.1242/dev.065540/-/DC1

References

Abrous, D. N., Koehl, M. and Le Moal, M. (2005). Adult neurogenesis: from precursors to network and physiology. *Physiol. Rev.* **85**, 523-569.
Altman, J. and Das, G. D. (1965). Autoradiographic and histological evidence of postnatal hippocampal neurogenesis in rats. *J. Comp. Neurol.* **124**, 319-335.
Alvarez-Buylla, A., Seri, B. and Doetsch, F. (2002). Identification of neural stem cells in the adult vertebrate brain. *Brain Res. Bull.* **57**, 751-758.
Beffert, U., Stolt, P. C. and Herz, J. (2004). Functions of lipoprotein receptors in neurons. *J. Lipid Res.* **45**, 403-409.
Bersenev, A., Wu, C., Balcerek, J. and Tong, W. (2008). Lnk controls mouse hematopoietic stem cell self-renewal and quiescence through direct interactions with JAK2. *J. Clin. Invest.* **118**, 2832-2844.
Blaiss, C. A., Yu, T. S., Zhang, G., Chen, J., Dimchev, G., Parada, L. F., Powell, C. M. and Kernie, S. G. (2011). Temporally specified genetic ablation of neurogenesis impairs cognitive recovery after traumatic brain injury. *J. Neurosci.* **31**, 4906-4916.
Bonaguidi, M. A., Wheeler, M. A., Shapiro, J. S., Stadel, R. P., Sun, G. J., Ming, G. L. and Song, H. (2011). In vivo clonal analysis reveals self-renewing and multipotent adult neural stem cell characteristics. *Cell* **145**, 1142-1155.
Bu, G. (2009). Apolipoprotein E and its receptors in Alzheimer's disease: pathways, pathogenesis and therapy. *Nat. Rev. Neurosci.* **10**, 333-344.
Cameron, H. A. and McKay, R. D. (2001). Adult neurogenesis produces a large pool of new granule cells in the dentate gyrus. *J. Comp. Neurol.* **435**, 406-417.
Chen, J., Kwon, C. H., Lin, L., Li, Y. and Parada, L. F. (2009). Inducible site-specific recombination in neural stem/progenitor cells. *Genesis* **47**, 122-131.
Christie, B. R. and Cameron, H. A. (2006). Neurogenesis in the adult hippocampus. *Hippocampus* **16**, 199-207.
Deguchi, K., Inoue, K., Avila, W. E., Lopez-Terrada, D., Antalffy, B. A., Quattrocchi, C. C., Sheldon, M., Mikoshiba, K., D'Arcangelo, G. and Armstrong, D. L. (2003). Reelin and disabled-1 expression in developing and mature human cortical neurons. *J. Neuropathol. Exp. Neurol.* **62**, 676-684.
Ding, H. K., Teixeira, C. M. and Frankland, P. W. (2008). Inactivation of the anterior cingulate cortex blocks expression of remote, but not recent, conditioned taste aversion memory. *Learn. Mem.* **15**, 290-293.
Doetsch, F. (2003). A niche for adult neural stem cells. *Curr. Opin. Genet. Dev.* **13**, 543-550.
Duan, X., Kang, E., Liu, C. Y., Ming, G. L. and Song, H. (2008). Development of neural stem cell in the adult brain. *Curr. Opin. Neurobiol.* **18**, 108-115.
Eidukevicius, R., Characiejus, D., Janavicius, R., Kazlauskaite, N., Pasukoniene, V., Mauricas, M. and Den Otter, W. (2005). A method to estimate cell cycle time and growth fraction using bromodeoxyuridine-flow cytometry data from a single sample. *BMC Cancer* **5**, 122.
Encinas, J. M., Vaahtokari, A. and Enikolopov, G. (2006). Fluoxetine targets early progenitor cells in the adult brain. *Proc. Natl. Acad. Sci. USA* **103**, 8233-8238.
Encinas, J. M., Michurina, T. V., Peunova, N., Park, J. H., Tordo, J., Peterson, D. A., Fishell, G., Koulakov, A. and Enikolopov, G. (2011). Division-coupled astrocytic differentiation and age-related depletion of neural stem cells in the adult hippocampus. *Cell Stem Cell* **8**, 566-579.
Eriksson, P. S., Perfilieva, E., Bjork-Eriksson, T., Alborn, A. M., Nordborg, C., Peterson, D. A. and Gage, F. H. (1998). Neurogenesis in the adult human hippocampus. *Nat. Med.* **4**, 1313-1317.
Frederiksen, K. and McKay, R. D. (1988). Proliferation and differentiation of rat neuroepithelial precursor cells in vivo. *J. Neurosci.* **8**, 1144-1151.
Fujita, S. C., Sakuta, K., Tsuchiya, R. and Hamanaka, H. (1999). Apolipoprotein E is found in astrocytes but not in microglia in the normal mouse brain. *Neurosci. Res.* **35**, 123-133.
Gage, F. H. (2002). Neurogenesis in the adult brain. *J. Neurosci.* **22**, 612-613.
Gilley, J. A., Yang, C. P. and Kernie, S. G. (2011). Developmental profiling of postnatal dentate gyrus progenitors provides evidence for dynamic cell-autonomous regulation. *Hippocampus* **21**, 33-47.
Gritti, A. and Bonfanti, L. (2007). Neuronal-glial interactions in central nervous system neurogenesis: the neural stem cell perspective. *Neuron Glia Biol.* **3**, 309-323.
Gundersen, H. J. (1980). Stereology – or how figures for spatial shape and content are obtained by observation of structures in sections. *Microsc. Acta* **83**, 409-426.
Guo, Y., Shi, D., Li, W., Liang, C., Wang, H., Ye, Z., Hu, L., Wang, H. Q. and Li, Y. (2008). Proliferation and neurogenesis of neural stem cells enhanced by cerebral microvascular endothelial cells. *Microsurgery* **28**, 54-60.
Herz, J. and Beffert, U. (2000). Apolipoprotein E receptors: linking brain development and Alzheimer's disease. *Nat. Rev. Neurosci.* **1**, 51-58.

Huang, Z. (2009). Molecular regulation of neuronal migration during neocortical development. *Mol. Cell. Neurosci.* **42**, 11-22.
Joksimovic, M., Yun, B. A., Kittappa, R., Anderegg, A. M., Chang, W. W., Taketo, M. M., McKay, R. D. and Awatramani, R. B. (2009). Wnt antagonism of Shh facilitates midbrain floor plate neurogenesis. *Nat. Neurosci.* **12**, 125-131.
Kempermann, G., Jessberger, S., Steiner, B. and Kronenberg, G. (2004). Milestones of neuronal development in the adult hippocampus. *Trends Neurosci.* **27**, 447-452.
Kim, D. H., Iijima, H., Goto, K., Sakai, J., Ishii, H., Kim, H. J., Suzuki, H., Kondo, H., Saeki, S. and Yamamoto, T. (1996). Human apolipoprotein E receptor 2. A novel lipoprotein receptor of the low density lipoprotein receptor family predominantly expressed in brain. *J. Biol. Chem.* **271**, 8373-8380.
Kim, S. U. and de Vellis, J. (2009). Stem cell-based cell therapy in neurological diseases: a review. *J. Neurosci. Res.* **87**, 2183-2200.
Kriegstein, A. and Alvarez-Buylla, A. (2009). The glial nature of embryonic and adult neural stem cells. *Annu. Rev. Neurosci.* **32**, 149-184.
Lagace, D. C., Whitman, M. C., Noonan, M. A., Ables, J. L., DeCarolis, N. A., Arguello, A. A., Donovan, M. H., Fischer, S. J., Farnbauch, L. A., Beech, R. D. et al. (2007). Dynamic contribution of nestin-expressing stem cells to adult neurogenesis. *J. Neurosci.* **27**, 12623-12629.
Lai, K., Kaspar, B. K., Gage, F. H. and Schaffer, D. V. (2003). Sonic hedgehog regulates adult neural progenitor proliferation in vitro and in vivo. *Nat. Neurosci.* **6**, 21-27.
Li, G., Bien-Ly, N., Andrews-Zwilling, Y., Xu, Q., Bernardo, A., Ring, K., Halabisky, B., Deng, C., Mahley, R. W. and Huang, Y. (2009). GABAergic interneuron dysfunction impairs hippocampal neurogenesis in adult apolipoprotein E4 knockin mice. *Cell Stem Cell* **5**, 634-645.
Li, Y., Luikart, B. W., Birnbaum, S., Chen, J., Kwon, C. H., Kernie, S. G., Bassel-Duby, R. and Parada, L. F. (2008). TrkB regulates hippocampal neurogenesis and governs sensitivity to antidepressive treatment. *Neuron* **59**, 399-412.
Lindvall, O. and Kokaia, Z. (2010). Stem cells in human neurodegenerative disorders-time for clinical translation? *J. Clin. Invest.* **120**, 29-40.
Machold, R., Hayashi, S., Rutlin, M., Muzumdar, M. D., Nery, S., Corbin, J. G., Gritli-Linde, A., Dellovade, T., Porter, J. A., Rubin, L. L. et al. (2003). Sonic hedgehog is required for progenitor cell maintenance in telencephalic stem cell niches. *Neuron* **39**, 937-950.
Mahley, R. W. (1988). Apolipoprotein E: cholesterol transport protein with expanding role in cell biology. *Science* **240**, 622-630.
Miles, D. K. and Kernie, S. G. (2008). Hypoxic-ischemic brain injury activates early hippocampal stem/progenitor cells to replace vulnerable neuroblasts. *Hippocampus* **18**, 793-806.
Ming, G. L. and Song, H. (2005). Adult neurogenesis in the mammalian central nervous system. *Annu. Rev. Neurosci.* **28**, 223-250.
Morrison, S. J., White, P. M., Zock, C. and Anderson, D. J. (1999). Prospective identification, isolation by flow cytometry, and in vivo self-renewal of multipotent mammalian neural crest stem cells. *Cell* **96**, 737-749.
Peng, Q., Masuda, N., Jiang, M., Li, Q., Zhao, M., Ross, C. A. and Duan, W. (2008). The antidepressant sertraline improves the phenotype, promotes neurogenesis and increases BDNF levels in the R6/2 Huntington's disease mouse model. *Exp. Neurol.* **210**, 154-163.
Pfrieger, F. W. (2003a). Cholesterol homeostasis and function in neurons of the central nervous system. *Cell. Mol. Life Sci.* **60**, 1158-1171.
Pfrieger, F. W. (2003b). Outsourcing in the brain: do neurons depend on cholesterol delivery by astrocytes? *BioEssays* **25**, 72-78.
Riquelme, P. A., Drapeau, E. and Doetsch, F. (2008). Brain micro-ecologies: neural stem cell niches in the adult mammalian brain. *Philos. Trans. R. Soc. Lond. B* **363**, 123-137.
Seaberg, R. M. and van der Kooy, D. (2002). Adult rodent neurogenic regions: the ventricular subependyma contains neural stem cells, but the dentate gyrus contains restricted progenitors. *J. Neurosci.* **22**, 1784-1793.
Seki, T. (2002). Hippocampal adult neurogenesis occurs in a microenvironment provided by PSA-NCAM-expressing immature neurons. *J. Neurosci. Res.* **69**, 772-783.
Seri, B., Garcia-Verdugo, J. M., Collado-Morente, L., McEwen, B. S. and Alvarez-Buylla, A. (2004). Cell types, lineage, and architecture of the germinal zone in the adult dentate gyrus. *J. Comp. Neurol.* **478**, 359-378.
Shapiro, H. M. (1981). Flow cytometric estimation of DNA and RNA content in intact cells stained with Hoechst 33342 and pyronin Y. *Cytometry* **2**, 143-150.
Shi, J., Miles, D. K., Orr, B. A., Massa, S. M. and Kernie, S. G. (2007). Injury-induced neurogenesis in Bax-deficient mice: evidence for regulation by voltage-gated potassium channels. *Eur. J. Neurosci.* **25**, 3499-3512.
Slezak, M. and Pfrieger, F. W. (2003). New roles for astrocytes: regulation of CNS synaptogenesis. *Trends Neurosci.* **26**, 531-535.
Suh, H., Deng, W. and Gage, F. H. (2009). Signaling in adult neurogenesis. *Annu. Rev. Cell Dev. Biol.* **25**, 253-275.
Tavazoie, M., Van der Veken, L., Silva-Vargas, V., Louissaint, M., Colonna, L., Zaidi, B., Garcia-Verdugo, J. M. and Doetsch, F. (2008). A specialized vascular niche for adult neural stem cells. *Cell Stem Cell* **3**, 279-288.
Trommsdorff, M., Gotthardt, M., Hiesberger, T., Shelton, J., Stockinger, W., Nimpf, J., Hammer, R. E., Richardson, J. A. and Herz, J. (1999). Reeler/Disabled-like disruption of neuronal migration in knockout mice lacking the VLDL receptor and ApoE receptor 2. *Cell* **97**, 689-701.
van Praag, H., Schinder, A. F., Christie, B. R., Toni, N., Palmer, T. D. and Gage, F. H. (2002). Functional neurogenesis in the adult hippocampus. *Nature* **415**, 1030-1034.
West, M. J. (1993). New stereological methods for counting neurons. *Neurobiol. Aging* **14**, 275-285.
Xu, Q., Bernardo, A., Walker, D., Kanegawa, T., Mahley, R. W. and Huang, Y. (2006). Profile and regulation of apolipoprotein E (ApoE) expression in the CNS in mice with targeting of green fluorescent protein gene to the ApoE locus. *J. Neurosci.* **26**, 4985-4994.
Yu, T. S., Dandekar, M., Monteggia, L. M., Parada, L. F. and Kernie, S. G. (2005). Temporally regulated expression of Cre recombinase in neural stem cells. *Genesis* **41**, 147-153.
Yu, T. S., Zhang, G., Liebl, D. J. and Kernie, S. G. (2008). Traumatic brain injury-induced hippocampal neurogenesis requires activation of early nestin-expressing progenitors. *J. Neurosci.* **28**, 12901-12912.
Zhao, C., Teng, E. M., Summers, R. G., Jr, Ming, G. L. and Gage, F. H. (2006). Distinct morphological stages of dentate granule neuron maturation in the adult mouse hippocampus. *J. Neurosci.* **26**, 3-11.
Zhao, C., Deng, W. and Gage, F. H. (2008). Mechanisms and functional implications of adult neurogenesis. *Cell* **132**, 645-660.